Formation of NH_3 and CH_2NH in Titan's upper atmosphere

Roger V. Yelle,[a] V. Vuitton,[b] P. Lavvas,[a] S. J. Klippenstein,[c] M. A. Smith,[ad] S. M. Hörst[a] and J. Cui[e]

Received 30th March 2010, Accepted 20th April 2010
DOI: 10.1039/c004787m

The large abundance of NH_3 in Titan's upper atmosphere is a consequence of coupled ion and neutral chemistry. The density of NH_3 is inferred from the measured abundance of NH_4^+. NH_3 is produced primarily through reaction of NH_2 with H_2CN, a process neglected in previous models. NH_2 is produced by several reactions including electron recombination of $CH_2NH_2^+$. The density of $CH_2NH_2^+$ is closely linked to the density of CH_2NH through proton exchange reactions and recombination. CH_2NH is produced by reaction of $N(^2D)$ and NH with ambient hydrocarbons. Thus, production of NH_3 is the result of a chain of reactions involving non-nitrile functional groups and the large density of NH_3 implies large densities for these associated molecules. This suggests that amine and imine functional groups may be incorporated as well in other, more complex organic molecules.

1. Introduction

Measurements of the composition of Titan's ionosphere provide a sensitive probe of the composition of the neutral atmosphere. Analysis of the ion mass spectrum reveals the presence of numerous nitrogen-bearing molecules.[1–3] In addition to nitriles, the chemistry of which has been well studied with photochemical models, the ionospheric measurements indicate substantial densities of $CH_2NH_2^+$ and NH_4^+, which in turn imply the presence of substantial quantities of CH_2NH and NH_3 in the upper atmosphere.[1–3] The chemistry of these species is important because the nitrogen functional groups (imines, amines, *etc.*) may be incorporated into larger organic molecules of biological interest, such as amino acids or nucleic acid bases.[4] We therefore present here an investigation into the photochemistry of non-nitrile nitrogenous species, constrained by Cassini observations of Titan's upper atmosphere.

The distributions of NH_4^+ and NH_3 and $CH_2NH_2^+$ and CH_2NH are closely related. One of the main chemical processes in Titan's ionosphere is proton exchange, where charge flows to the species with the largest proton affinity.[2,3,5] Thus, NH_4^+ and $CH_2NH_2^+$ are created by reaction of NH_3 and CH_2NH with other protonated molecules, while recombination of NH_4^+ and $CH_2NH_2^+$ produce NH_3 and CH_2NH. The densities of the neutral and protonated species are tightly connected by this chemistry and the observed ion densities along with a model for the chemistry predict that NH_3 and CH_2NH are present in Titan's upper atmosphere

[a]*Department of Planetary Sciences, University of Arizona, Tucson, AZ, 85721, USA*
[b]*Laboratoire de Planétogie de Grenoble, Université J. Fourier, Grenoble, France*
[c]*Chemical Sciences and Engineering Division, Argonne National Laboratory, Argonne, IL, 60439, USA*
[d]*Department of Chemistry and Biochemistry, University of Arizona, Tucson, AZ, 85721, USA*
[e]*Department of Physics, Imperial College, Prince Consort Road, London, SW7 2BW, U.K.*

with a mole fraction of several ppm at an altitude of 1100 km, near the ionospheric peak.[1–3]

The presence of several ppm of NH_3 in Titan's upper atmosphere was not predicted by photochemical models.[6–11] The NH_3 mole fraction in the stratosphere must be much smaller than in the upper atmosphere, because at several ppm spectral emission features would be apparent, but have not been seen; thus, the mole fraction of NH_3 must increase with altitude and there is a flux of NH_3 from the upper to lower atmosphere. This indicates that NH_3 is formed in the upper atmosphere. The situation is similar to that of benzene on Titan, which has a mole fraction of several ppm near 1000 km and is synthesized by chemistry in the ionosphere.[12] Here, we show that NH_3 is synthesized by a combination of neutral and ion chemistry in the upper atmosphere. Our investigation also predicts significant levels of N-bearing radicals in Titan's upper atmosphere.

2. Observations

Measurements of the ion densities in Titan's upper atmosphere have been described extensively by Cui *et al.*[13] and Cui *et al.*[14] and we use essentially the same data set here. The ion densities depend on the spacecraft potential and we use the procedure outlined in Cui *et al.*[13] to correct for this effect. The observations were recorded during 40 flybys of the Cassini spacecraft through Titan's upper atmosphere. These data are collected along the spacecraft track over which altitude, latitude, longitude, solar zenith angle, *etc.* all vary considerably. Cui *et al.*[14] averaged and interpolated these data set to produce mean altitude profiles of constituent densities for several ranges of solar zenith angle. Binning by solar zenith angle is motivated by the fact that ion and electron densities are observed to be well correlated with solar input.[13,15] Fig. 1 shows the mean NH_4^+ and $CH_2NH_2^+$ densities for the dayside and nightside. As pointed out in Cui *et al.*,[13] NH_4^+ displays little diurnal variation while $CH_2NH_2^+$ actually has a slightly larger density on the nightside than the dayside. These characteristics are related to the fact that both species are terminal ions, lost primarily through electron recombination, and characterized by relatively long time constants.

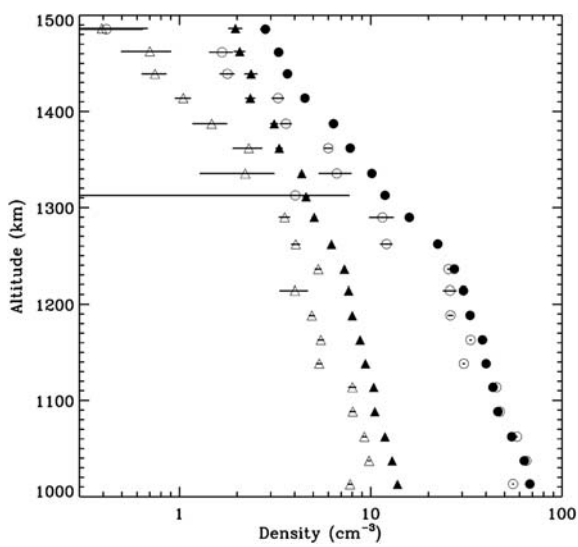

Fig. 1 Circles and triangles represent the $CH_2NH_2^+$ and NH_4^+ densities, respectively. Filled symbols represent average dayside values and open symbols average nightside values. The error bars include only uncertainties due to counting statistics.

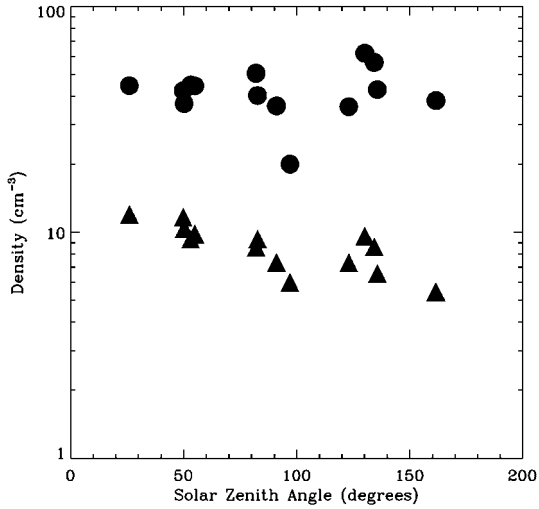

Fig. 2 Variation of $CH_2NH_2^+$ (circles) and NH_4^+ (triangles) with solar zenith angle.

As the ionosphere moves to larger solar zenith angles because of the rotation of the satellite and strong winds, the short-lived ions transfer their charge to longer-lived ions through ion–neutral reactions. Chemical production of terminal ions therefore continues on the nightside, explaining how some ions can be more abundant at night than during the day.[13]

Fig. 2 shows the densities of NH_4^+ or $CH_2NH_2^+$ for each of the passes used in this analysis. The pass-to-pass variations are fairly small, although $CH_2NH_2^+$ does exhibit some outliers. The NH_4^+ data shows a small but clear trend of decreasing density with increasing solar zenith angle. The $CH_2NH_2^+$ shows no clear correlation with solar zenith angle. The lack of strong variability in the data implies that they can be adequately interpreted with a 1D model.

The identification of the signals at $m/z = 18$ and 30 as NH_4^+ and $CH_2NH_2^+$ is discussed by Vuitton *et al.*,[2] Vuitton *et al.*,[3] and Cravens *et al.*[1] For $m/z = 18$, the only alternative to NH_4^+ is H_2O^+; however, the main loss for H_2O^+ is reaction with neutrals to produce H_3O^+, while H_3O^+ recombines with electrons at a slower rate. Thus, the lack of a strong signal at $m/z = 19$, implies a negligible contribution at $m/z = 18$ from H_2O^+. For $m/z = 30$, the options are $CH_2NH_2^+$, NO^+, and $C_2H_6^+$. The latter species is a radical ion and therefore highly reactive and chemical models imply that it should have a small density.[3] NO^+ is stable, but should also have a low density, essentially because the O density in Titan's atmosphere is low.[3]

3. Chemistry

Fig. 3 illustrates the chemical pathways leading to production of NH_3. To keep the diagram simple and readable we show only major chemical reactions. There are two main routes to production of NH_3. The lower path relies exclusively on addition of H to NH_x^+ through reactions with CH_4 and H_2 and has been suggested previously by Atreya.[16] In fact, there is a very tight connection between NH_3 and NH_4^+ because the proton exchange reaction and recombination both proceed rapidly; however, this does not represent a change in the NH_3 abundance, but only a change in its form (protonated or not). The rate for the ion chemistry channel is not limited by production or recombination of NH_4^+, but production of NH_2^+ through reactions of N^+ with H_2 and NH^+ with CH_4. The former reaction proceeds rapidly; however, most of the NH^+ formed by reaction of N^+ with H_2 reacts with N_2 to form N_2H^+,

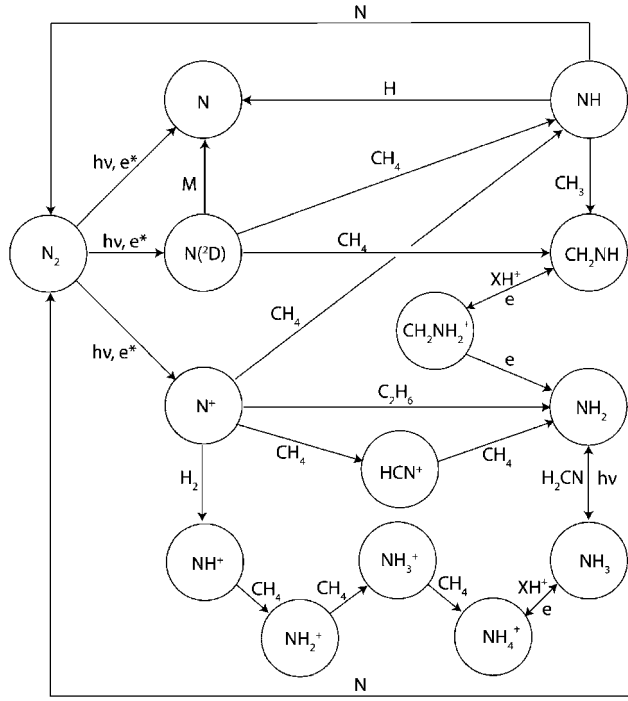

Fig. 3 Chemical pathways for production of NH_3 and CH_2NH.

which then reacts with CH_4 and HCN to produce CH_5^+ and $HCNH^+$. This effectively short-circuits production of NH_3 through this sequence. Calculations described in sections 5 and 6 show that this channel is a minor source of NH_3 on Titan.

The other pathway shown in Fig. 3 relies on conversion of NH_2 to NH_3. The NH_2 radical does not react with any of the stable molecules in the upper atmosphere (N_2, CH_4, C_2H_2, C_2H_4, *etc.*). The primary chemical loss for NH_2 must be reaction with other radicals. H, CH_3 and N are the most abundant radicals in Titan's upper atmosphere; however, NH_2 does not undergo two-body reactions with H. Three-body reactions do occur, but happen at too high a pressure to affect the ionosphere. NH_2 does react with N, leading to production of N_2, which, along with NH + N $\rightarrow$ N_2 + H, is a main channel for loss of active nitrogen on Titan. NH_2 does undergo a three-body reaction with CH_3, producing CH_3NH_2, but the two-body reaction has not been measured. The H_2CN radical also has a fairly large abundance in the upper atmosphere. It is produced by reaction of N and CH_3, two of the main products from photodissociation of N_2 and CH_4. H_2CN is also the precursor of HCN, the most abundant nitrile in Titan's atmosphere. The difficulty with this proposition is that the reaction rate for $NH_2 + H_2CN \rightarrow NH_3 + HCN$ has not been measured. Nevertheless the reaction is exothermic and, as a radical–radical reaction, should proceed rapidly. In section 4 we present calculations of the rate coefficient based on transition state theory that show that it is quite rapid. This implies that $NH_2 + H_2CN \rightarrow NH_3 + HCN$ is indeed the dominant pathway for production of NH_3 in Titan's upper atmosphere.

With this approach, to produce NH_3, we first need NH_2. The amino radical is also produced by two reactions, but both involve ionospheric chemistry, recombination ($CH_2NH_2^+ + e \rightarrow CH_2 + NH_2$) and ion–neutral reaction ($N^+ + C_2H_4 \rightarrow NH_2 + C_2H_2^+$ or $N^+ + C_2H_6 \rightarrow NH_2 + C_2H_4^+$). N^+ for the latter channels is produced

directly from dissociative ionization of N_2 by solar photons and suprathermal electrons. $CH_2NH_2^+$ can be produced by proton exchange reactions with any of the protonated species in Titan's ionosphere. There are many candidates because the ionosphere is composed predominantly of such ions,[2,3] the most abundant of which is $HCNH^+$. CH_2NH has a proton affinity of 853.7 kJ mol^{-1}, which is larger than that for most of the nitrile species (including HCN) and all of the hydrocarbon species in Titan's atmosphere;[3] therefore all of these species will react with CH_2NH to produce $CH_2NH_2^+$. These considerations indicate that there is a direct connection among the abundances of $CH_2NH_2^+$, CH_2NH, NH_4^+, and NH_3.

Methanimine on Titan is produced by two reactions: $NH + CH_3 \rightarrow CH_2NH + H$ and $N(^2D) + CH_4 \rightarrow CH_2NH + H$. The metastable $N(^2D)$ atoms, which are produced by photo or electron impact dissociation of N_2, plays an essential role in the nitrogen chemistry on Titan.[17] NH is produced from $N(^2D)$ through reaction with CH_4 and from reaction of N^+ with CH_4. CH_2NH may also be recycled through electron recombination of $CH_2NH_2^+$, though the products of this reaction have never been measured. This has a small effect on the chemistry because CH_2NH simply cycles between neutral and protonated forms until NH_2 is produced.

There are two ways that production of NH_2 might not follow production of CH_2NH. One possibility is if recombination of $CH_2NH_2^+$ produces HCN. This is energetically possible, but remains to be verified by theory or experiment. The other possibility is that CH_2NH is photo-dissociated into HCN + 2H. In fact, according to Nguyen *et al.*[18] this is the dominant channel for dissociation. We consider both these possibilities in our numerical model, described below. Neither alter the conclusion that NH_3 is produced primarily from NH_2. Photolysis of NH_3 (R4) also produces NH_2, but this is important primarily at lower altitudes.

4. Calculation of the rate coefficient for $NH_2 + H_2CN \rightarrow NH_3 + HCN$

The mechanism for the reaction of NH_2 with H_2CN was explored at the QCISD(T)/CBS//B3LYP/6-311++G(d,p) level, and is illustrated in Fig. 4. In these calculations, the rovibrational properties of the stationary points were mapped out with B3LYP (Becke-3 Lee–Yang–Parr) density functional theory employing the 6-311++G(d,p) basis set. Complete basis set (CBS) RQCISD(T) (spin-restricted quadratic

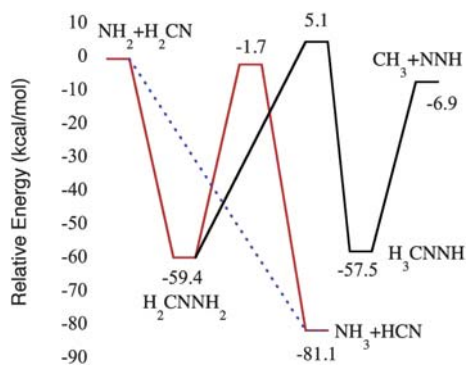

Fig. 4 Schematic plot of the potential energy surface for the reaction of NH_2 with H_2CN. The numbers denote QCISD(T)/CBS//B3LYP/6-311++G(d,p) zero-point corrected energies (in kcal mol^{-1}) relative to reactants. The blue dotted line represents a direct abstraction pathway, the red solid line denotes an addition–elimination pathway to form NH_3 + HCN, and the black solid line denotes a pathway that leads to the formation of CH_3 + NNH. Other pathways, to produce H_2 + H_2CNN for example, involve high energy saddle points and so are not shown.

configuration interaction with perturbative inclusion of triplets) energy estimates are then obtained from basis set extrapolation of calculations with Dunning's correlation-consistent polarized-valence triple-zeta (cc-pVTZ) and quadruple-zeta (cc-pVQZ) basis sets;[19] Kendall *et al.*[20]).

The plot in Fig. 4 indicates that, at least at low temperature, the NH_2 + H_2CN reaction will involve two primary pathways. One pathway involves the simple addition to form an H_2CNNH_2 adduct, which may then proceed on to NH_3 + HCN *via* a tight transition state at −1.7 kcal mol^{-1}. Alternatively, further collisions may simply stabilize the initial adduct. A second pathway involves direct abstraction to immediately form NH_3 + HCN. A third pathway, with a saddle point at 5.1 kcal mol^{-1} for isomerization of H_2CNNH_2 to $HCNNH_3$, is sufficiently high in energy that it will make little contribution under the conditions in Titan's atmosphere.

The simple doublet radical nature of each of the reactants suggests that the addition reaction will be barrierless. Meanwhile, the fact that the transition state for the isomerization from H_2CNNH_2 to NH_3 + HCN lies below the reactants suggests that the overall addition–elimination reaction should be quite rapid at low temperatures and low pressures. At higher temperatures it may be somewhat slower due to the low entropy for the isomerization transition state. The highly exothermic nature of the direct abstraction suggests that the abstraction channel is also likely to be barrierless and to occur with a rate coefficient approaching the collision limit.

Multi-reference second order perturbation theory (CASPT2) calculations indicate that both the simple addition and direct abstraction channels are indeed barrierless, as illustrated in Fig. 5. These CASPT2/CBS calculations employ a 4-electron 4-orbital (4e,4o) active space consisting of the NH_2 and H_2CN radical orbitals in addition to the H_2CN π, π^* orbitals. The plots are for the interaction between NH_2 and H_2CN as a function of either the NH (for abstraction) or NN (for addition) separation, with the two radicals in fixed orientations (appropriate for either the abstraction or the addition channels) and with their fixed asymptotic structures. Allowing for relaxation of the orientations and the internal structures of the reacting moieties would simply yield modestly more attractive interaction potentials for these two channels. Clearly, the addition and direct abstraction pathways are indeed barrierless.

Here we implement the direct variable-reaction coordinate (VRC) transition state theory (TST) approach[21–24] in predicting the kinetics for the addition and abstraction

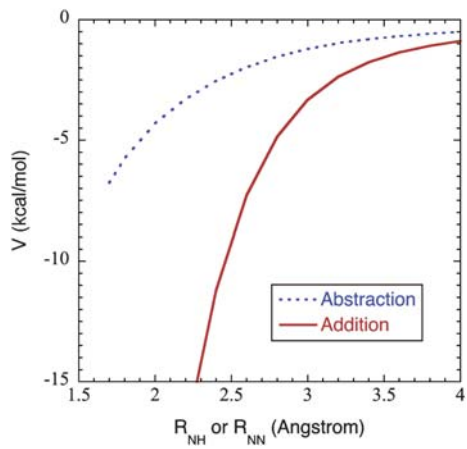

Fig. 5 Plot of the CASPT2(4e,4o)/CBS interaction potentials for the abstraction (blue dashed line) and addition (red solid) channels in the NH_2 + H_2CN reaction.

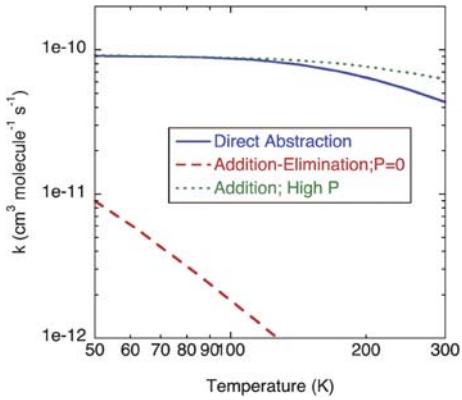

Fig. 6 Plot of the temperature dependence of the rate coefficients for direct abstraction (blue solid line), for addition–elimination (red dashed line), and for addition in the high pressure limit (green dotted line) in the NH_2 + H_2CN reaction.

channels. The VRC-TST approach was designed to accurately treat the effect of anharmonicities and mode couplings for such barrierless reactions, and has been shown to yield accurate kinetic predictions for various radical–radical reactions.[25,26] Here we employ direct CASPT2(4e,4o) calculations of the orientation dependence of the interaction energies. These calculations were done for both the cc-pVDZ and aug-cc-pVDZ basis sets. The final estimates for the interaction energies are obtained by adding one-dimensional CASPT2 complete basis set and geometry relaxation corrections. The kinetic predictions for the corrected CASPT2/cc-pvdz and CASPT2/aug-cc-pvdz samplings differed by only a few percent. The results reported here employ the average of these two results and incorporate a dynamical correction factor of 0.85, which is based on dynamical evaluation of the transition state recrossing for the related CH_3 + CH_3 recombination reaction.[26]

For the addition process, it is also important to consider the branching between stabilization, elimination, and back dissociation from the initially formed H_2CNNH_2 adduct. Sample master equation simulations suggest that stabilization of the complex is insignificant for the temperature and pressures of relevance to Titan's upper atmosphere. In this case, the addition–elimination rate constant is equal to its collisionless limit value, essentially independent of pressure.

The CASPT2 calculations were done using the formalism of Celani and Werner[27] as implemented in the MOLPRO08 electronic structure software package. The QCISD(T) calculations also use the MOLPRO08 package while the B3LYP calculations were done with the GAUSSIAN98 software package.[28–31]

The temperature dependent rate coefficients for the direct abstraction, high pressure addition, and addition–elimination reactions are plotted in Fig. 6 Interestingly, the direct abstraction and high pressure addition rate coefficients are roughly equivalent. However, the addition–elimination rate coefficient is greatly reduced from the high pressure addition rate coefficient even at a temperature of 50 K. Apparently, the tight transition state for the isomerization from H_2CNNH_2 to NH_3 + HCN is a significant bottleneck down to rather low temperature. The modified Arrhenius expression, $5.42 \times 10^{-11}(T/300)^{-1.06} \exp(-60.8/T)$ cm^3 s^{-1}, with T in K, reproduces the present predictions for the total rate coefficient for formation of NH_3 + HCN in the low pressure limit over the 40 to 400 K temperature range.

5. Photochemical model

The model used in this investigation is adapted from several elements used in previous investigations. The chemistry of N-bearing molecules is closely coupled

to the ion chemistry in Titan's upper atmosphere. We therefore model the ion and neutral chemistry in a coupled, self-consistent manner. This is an improvement over the approach taken in Vuitton *et al.*,[12] where the ionosphere was treated as a source for neutral molecules, but the influence of the neutral composition on the ionosphere was not included self-consistently. The ionospheric part of the model is based on the reaction list described by Vuitton *et al.*[3] Some aspects of the neutral photochemistry as well as the treatment of eddy and molecular diffusion are discussed in Hörst *et al.*[32] The neutral N chemistry is adapted largely from Lavvas *et al.*,[33] with important additions discussed below. Our calculations extend up to 1500 km but we emphasize the region near the ionospheric peak at 1100 km and therefore neglect ion diffusion and assume local chemical equilibrium. This assumption is accurate near the ionospheric peak but breaks down near ~1250 km.[14] This should not have any effect on our conclusions. Diffusion is included for all neutral species. Diffusion coefficients for most species come from Mason and Marrero.[34] For NH_3–N_2 diffusion we use the coefficients from Massman.[35] No data were found for CH_2NH–N_2 diffusion coefficients, so we assume the value is equal to that for C_2H_4–N_2, scaled by the square-root of the reduced mass. The eddy diffusion profile is taken from Yelle *et al.*[36]

Characteristics of the background neutral atmosphere used in our calculations are shown in Fig. 7 and 8. The neutral densities and temperatures are based on Cassini INMS data[13,37] and the electron temperature from the Langmuir probe channel of the Cassini RPWS experiment.[15] Hydrocarbon abundances are based on our photochemical calculations[12] and are in good agreement with observational constraints.[64] The model used here is appropriate for northern mid-latitudes.

Table 1 presents the important reactions for this investigation. When available, reaction rate data are taken from the literature, but in several cases no measurements are available and rates coefficients are estimated. The sensitivities of our results to these assumptions are discussed in section 6. In this work we are interested primarily in the upper atmosphere, where two-body reactions dominate. Our nitrogen reaction

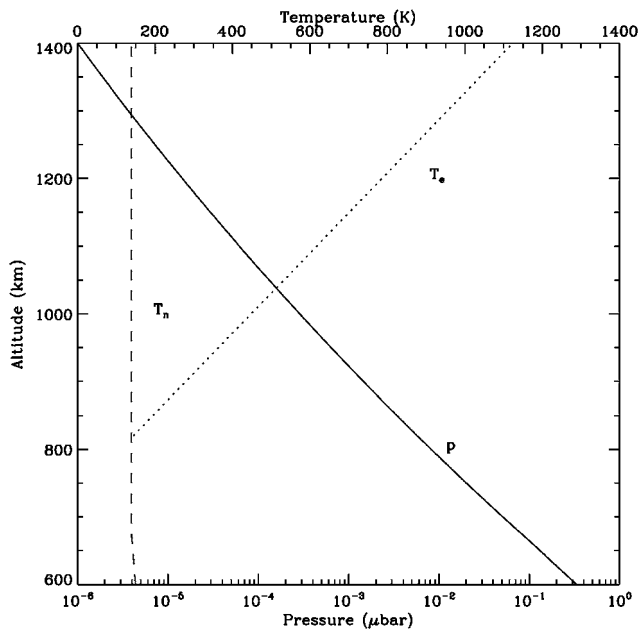

Fig. 7 The altitude variation of pressure, neutral temperature, and electron temperature used in the photochemical calculations.

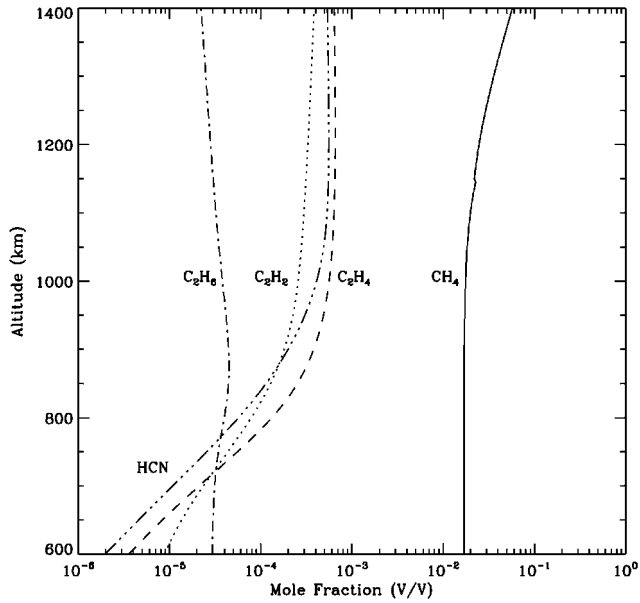

Fig. 8 Mole fractions of stable neutral species used in the photochemical calculations.

list therefore emphasizes two-body processes and likely neglects some three-body reactions that could be important in the stratosphere.

The model is one dimensional and uses globally averaged photolysis rates. This is justified by the fact that the observed diurnal variations of NH_4^+ and $CH_2NH_2^+$ are quite small (Fig. 2); moreover, latitudinal and diurnal variations in the background atmosphere near 1100 km are small.[37] Also, we are interested here primarily in identifying the chemical pathways for production of NH_3 and CH_2NH, rather than precise modeling of their density profiles. A 1D model is adequate for this purpose. The complexity and computational expense of a 3D model, along with the associated uncertainty in the circulation patterns, suggest that the 3D models be deferred until the chemistry is well established and the dynamics of the upper atmosphere better understood.

Dissociation and ionization of N_2 and CH_4 are modeled in detail, including both photon and electron induced processes. Neutral photodissociation of N_2 is calculated making use of newly determined high-resolution cross sections.[62,63] The supra-thermal electron distribution is calculated based on a local energy deposition approximation that has been validated through comparison with a supra-thermal electron transport code. The reader is referred to [17] for an in depth discussion of the photolysis of CH_4 and N_2.

Several of the rate coefficients in Table 1 had to be estimated, because of a lack of laboratory measurements or theoretical calculations. In section 4, we describe our calculations of the rate coefficient for $NH_2 + H_2CN$. The most important reaction for which we are missing required data is electron recombination of $CH_2NH_2^+$ (R19–R21). Based on analogy with electron recombination of other complex hydrocarbon ions, we expect the rate coefficient to be large and adopt in our baseline model a value of 2.1×10^{-6} cm^3 s^{-1} for the net rate with equal probabilities for three branches: $CH_2NH + H$, $CH_2 + NH_2$, and $HCN + H + H_2$. This value is chosen because it provides the best match between predicted and observed densities of $CH_2NH_2^+$; however, we also consider in the next section the sensitivity of our model to the value assumed for the rate coefficient and branching ratios. Also uncertain is the photolysis rate for CH_2NH.[33] The products have been estimated theoretically,[18]

Table 1 Selected reactions

	Reaction	Rate coefficient[a]	Reference
Photolysis			
R1	$N_2 + h\nu \rightarrow N^+ + N + e$	4.9×10^{-10}	38, 39
R2	$N_2 + h\nu \rightarrow N(^2D) + N$	2.2×10^{-9}	17
R3	$CH_2NH + h\nu \rightarrow HCN + H + H$	1.1×10^{-8}	18, 40
R4	$NH_3 + h\nu \rightarrow NH_2 + H$	8.2×10^{-7}	41, 42
Ion reactions			
R5	$N^+ + CH_4 \rightarrow CH_3^+ + NH$	5.75×10^{-9}	43
R6	$\rightarrow CH_4^+ + N$	5.75×10^{-10}	43
R7	$\rightarrow HCN^+ + H_2 + H$	1.15×10^{-10}	43
R8	$N^+ + H_2 \rightarrow NH^+ + H$	5.00×10^{-10}	43
R9	$N^+ + C_2H_4 \rightarrow C_2H_3^+ + NH$	3.25×10^{-10}	44, 43
R10	$\rightarrow C_2H_2^+ + NH_2$	1.30×10^{-10}	44, 45
R11	$N^+ + C_2H_6 \rightarrow C_2H_3^+ + NH_3$	2.50×10^{-10}	44, 45
R12	$HCN^+ + CH_4 \rightarrow C_2H_3^+ + NH_2$	1.27×10^{-10}	43
R13	$HCNH^+ + CH_2NH \rightarrow CH_2NH_2^+ + HCN$	2.7×10^{-9}	46
R14	$C_2H_5^+ + CH_2NH \rightarrow CH_2NH_2^+ + C_2H_4$	2.7×10^{-9}	3
R15	$CH_5^+ + CH_2NH \rightarrow CH_2NH_2^+ + CH_4$	3.0×10^{-9}	3
R16	$HCNH^+ + NH_3 \rightarrow NH_4^+ + HCN$	2.30×10^{-9}	43
R17	$C_2H_5^+ + NH_3 \rightarrow NH_4^+ + C_2H_4$	2.00×10^{-9}	43
R18	$HC_3NH^+ + NH_3 \rightarrow NH_4^+ + HC_3N$	2.09×10^{-9}	47
R19	$CH_2NH_2^+ + e \rightarrow CH_2NH + H$	$0.5–1.4 \times 10^{-6}(300/Te)^{0.7}$	Estimated (see text)
R20	$\rightarrow CH_2 + NH_2$	$0.5–1.4 \times 10^{-6}(300/Te)^{0.7}$	Estimated (see text)
R21	$\rightarrow HCN + H + H_2$	$0.5–1.4 \times 10^{-6}(300/Te)^{0.7}$	Estimated (see text)
R22	$NH_4^+ + e \rightarrow NH_3 + H$	$8.02 \times 10^{-7}(300/Te)^{0.605}e^{-510/Te}$	48
R23	$\rightarrow NH_2 + H + H$	$1.23 \times 10^{-7}(300/Te)^{0.605}e^{-510/Te}$	48
Neutral reactions			
R24	$H + CH_2NH \rightarrow H_2CN + H_2$	4.0×10^{-14}	49
R25	$N + CH_3 \rightarrow H_2CN + H$	$4.3 \times 10^{-10}e^{-420/T}$	50

Table 1 (*Contd.*)

	Reaction	Rate coefficient[a]	Reference
R26	$N + H_2CN \rightarrow HCN + NH$	$1.0 \times 10^{-10} e^{-200/T}$	51
R27	$N(^2D) \rightarrow N + hv$	2.3×10^{-5}	52
R28	$N(^2D) + N_2 \rightarrow N + N_2$	1.7×10^{-14}	53
R29	$\rightarrow CH_2NH + H$	$3.84 \times 10^{-11} e^{-750/T}$	53
R30	$\rightarrow NH + CH_3$	9.6×10^{-12}	53
R31	$N(^2D) + H_2 \rightarrow N + H_2$	2.28×10^{-12}	54
R32	$\rightarrow NH + H$	$4.2 \times 10^{-11} e^{-880/T}$	53
R33	$N(^2D) + C_2H_2 \rightarrow HC_2N + H$	$1.6 \times 10^{-10} e^{-270/T}$	55, 53
R34	$N(^2D) + C_2H_4 \rightarrow CH_3CN + H$	4.4×10^{-11}	53
R35	$N(^2D) + C_2H_6 \rightarrow NH + C_2H_5$	3.8×10^{-12}	53
R36	$N(^2D) + HCN \rightarrow N_2 + CH$	$1.6 \times 10^{-10} e^{-270/T}$	Estimated, based on R35
R37	$NH + C_2H_2 \rightarrow HC_2N + H_2$	$2.01 \times 10^{-9} T^{-1.07}$	57
R38	$NH + C_2H_4 \rightarrow CH_3CN + H_2$	$2.3 \times 10^{-12} (T/300)^{-1.09}$	57
R39	$NH + C_2H_6 \rightarrow C_2H_5N + H_2$	6.8×10^{-12}	57
R40	$NH + C_4H_2 \rightarrow C_4HN + H_2$	$8.24 \times 10^{-9} T^{-1.23}$	57
R41	$NH + H \rightarrow N + H_2$	$3.12 \times 10^{-16} T^{1.55} e^{-103/T}$	56
R42	$NH + CH_3 \rightarrow CH_2NH + H$	$3.12 \times 10^{-16} T^{1.55} e^{-103/T}$	Estimated, based on R43
R43	$NH + N \rightarrow N_2 + H$	2.49×10^{-11}	58
R44	$NH + NH \rightarrow NH_2 + N$	$9.9 \times 10^{-22} T^{2.89} e^{1021/T}$	59
R45	$NH_2 + N \rightarrow N_2 + H + H$	1.2×10^{-10}	60
R46	$NH_2 + NH_2 \rightarrow N_2H_4$	$8.97 \times 10^{-20} T^{-3.9}$	61
R47	$NH_2 + H2CN \rightarrow NH_3 + HCN$	$5.42 \times 10^{-11} (T/300)^{-1.06} e^{-60.8/T}$	This work

[a] Photolysis rates are diurnally averaged optically thin values at 9.5 AU. Units are s^{-1}. Other rate coefficients have units of $cm^3\ s^{-1}$.

ART ■ C004787M

but the cross section has only been measured over a small wavelength range.[40] Using this information we estimate a rate at 1 AU of 1.0×10^{-6} s^{-1}, but also consider models with other values.

6. Model results

Calculated densities for a selection of ion and neutral species in the baseline model are shown in Fig. 9, along with the measured densities of NH_4^+ and $CH_2NH_2^+$. Agreement is adequate over most of the altitude range and sufficient to conclude that the primary production and loss mechanisms for NH_3 and CH_2NH have been properly identified. Radical species, N, H_2CN, NH and $N(^2D)$ dominate near the ionospheric peak at ~1100 km. At lower altitudes these give way to the more stable species, NH_3 and CH_2NH.

Reactions rates shown in Fig. 10a–d, can be used to follow the chemical cycles. NH is produced primarily by ion chemistry through R5: $N^+ + CH_4 \rightarrow CH_3^+ + NH$ and lost through reaction with C_2H_2 and C_2H_4 (R37, R38) which produce nitrile species and through reaction with CH_3, which produces CH_2NH (R42). The column-integrated rate of NH production through R5 is 2.6×10^7 cm^2 s^{-1} and roughly 40% of the NH so produced results in CH_2NH production through R42. There is no direct route of any significance from NH to NH_2, but we discuss below how production of CH_2NH can lead to NH_2. Loss due to diffusion is not significant for NH and the density is close to photochemical equilibrium.

CH_2NH plays a dual role in the chemistry as both an intermediary for NH_2 production and as an important, stable product itself. As shown in Fig. 10b, CH_2NH is produced by reaction of NH with CH_3 (R42) and by electron recombination of $CH_2NH_2^+$ (R19). However, $CH_2NH_2^+$ is produced primarily by proton transfer reactions of several species with CH_2NH (R13–15), so production of CH_2NH through R19 is a recycling of CH_2NH rather than production of new molecules. Electron recombination of $CH_2NH_2^+$ may also produce CH_2 and NH_2 (R20), which eventually leads to formation of NH_3. At lower altitudes, CH_2NH is lost by reaction with H (R24), which produces H_2CN. The H_2CN is eventually converted into HCN,

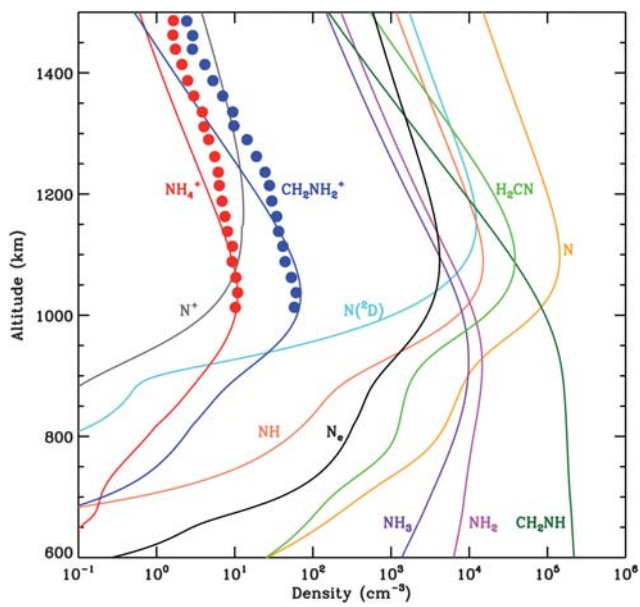

Fig. 9 Densities of significant nitrogen-bearing species calculated in the baseline model. The data points represent INMS measurements, solid lines the model calculations.

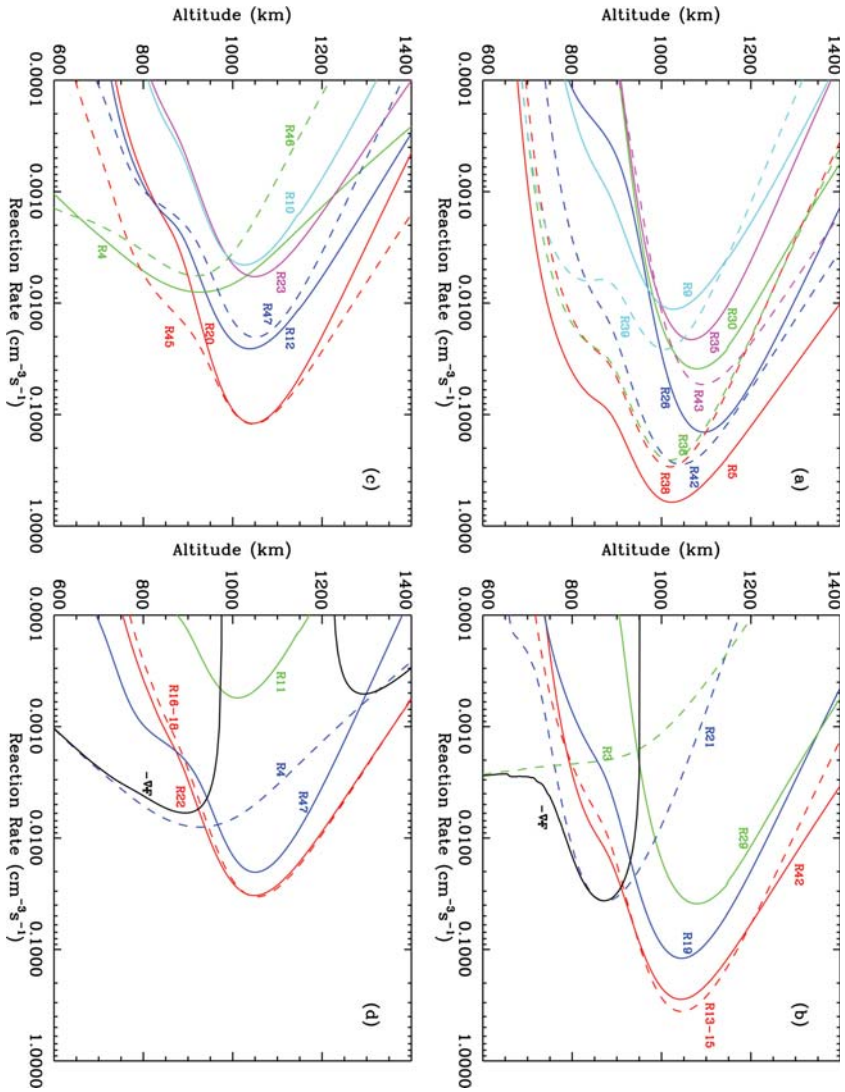

Fig. 10 Primary production and loss rates in our model. Solid and dashed curves represent production and loss, respectively. $-\nabla \cdot F$ represents local production due to diffusion. Labels for other curves refer to Table 1. Panels a–d show the dominant production and loss processes for a: NH, b: CH_2NH, c: NH_2, and d: NH_3.

and also aids in the production of NH_3. The column-integrated rate for R20 is 4.2×10^6 cm^2 s^{-1}, about 40% of the value for R42.

NH_2 is produced by reaction of HCN^+ with CH_4 (R12), in addition to R20. The former reaction contributes about 25% to the net rate and the latter 75%. The dominant loss process is reaction with N (R45), that produces N_2, destroying active nitrogen. The second most important loss process is reaction with H_2CN, which produces NH_3 (R47). In total, 81% of the NH_2 produced goes back to N_2 and 11% is converted to NH_3. The remaining 8% is converted to N_2H_4 by reaction with itself (R46). At lower altitudes, NH_2 is produced by photolysis of NH_3 (R4). The higher densities at lower altitude favor three-body recombination and the NH_2 produced from R4 is converted into N_2H_4.

Table 2 Model runs

Model	k_{47}/cm^3 s^{-1}	k_{19}/cm^3 s^{-1}	k_{20}/cm^3 s^{-1}	k_{21}/cm^3 s^{-1}	J_3/s^{-1}
A	$5.42 \times 10^{-11}(T/300)^{-1.06}e^{-60.8/T}$	$7.0 \times 10^{-7}(300/Te)^{0.7}$	$7.0 \times 10^{-7}(300/Te)^{0.7}$	$7.0 \times 10^{-7}(300/Te)^{0.7}$	10^{-6}
B	$3.61 \times 10^{-11}(T/300)^{-1.06}e^{-60.8/T}$	$7.0 \times 10^{-7}(300/Te)^{0.7}$	$7.0 \times 10^{-7}(300/Te)^{0.7}$	$7.0 \times 10^{-7}(300/Te)^{0.7}$	10^{-6}
C	$8.13 \times 10^{-11}(T/300)^{-1.06}e^{-60.8/T}$	$7.0 \times 10^{-7}(300/Te)^{0.7}$	$7.0 \times 10^{-7}(300/Te)^{0.7}$	$7.0 \times 10^{-7}(300/Te)^{0.7}$	10^{-6}
D	$5.42 \times 10^{-11}(T/300)^{-1.06}e^{-60.8/T}$	$5.0 \times 10^{-7}(300/Te)^{0.7}$	$5.0 \times 10^{-7}(300/Te)^{0.7}$	$5.0 \times 10^{-7}(300/Te)^{0.7}$	10^{-6}
E	$5.42 \times 10^{-11}(T/300)^{-1.06}e^{-60.8/T}$	$1.4 \times 10^{-6}(300/Te)^{0.7}$	$1.4 \times 10^{-6}(300/Te)^{0.7}$	$1.4 \times 10^{-6}(300/Te)^{0.7}$	10^{-6}
F	$5.42 \times 10^{-11}(T/300)^{-1.06}e^{-60.8/T}$	$7.0 \times 10^{-7}(300/Te)^{0.7}$	$7.0 \times 10^{-7}(300/Te)^{0.7}$	0	10^{-6}
G	$5.42 \times 10^{-11}(T/300)^{-1.06}e^{-60.8/T}$	$7.0 \times 10^{-7}(300/Te)^{0.7}$	$7.0 \times 10^{-7}(300/Te)^{0.7}$	$7.0 \times 10^{-7}(300/Te)^{0.7}$	10^{-7}

As shown in Fig. 10d, there is a precise balance between production of NH_3 by electron recombination of NH_4^+ and loss due to reaction with protonated ions, especially $HCNH^+$, $C_2H_5^+$, and CH_5^+ (R16–18). The balance reflects the fact that these reactions are not destroying NH_3 but only changing its form from the neutral to the protonated ion and back. True production of NH_3 occurs primarily through R47; thus, NH_3 follows directly from NH_2. Production through this channel is 25 times larger than from NH_3^+ considered in previous models.[16] Photolysis of NH_3 also produces NH_2, but this process is unimportant near 1100 km, although it becomes the dominant loss process at lower altitudes. The most likely fate of NH_2 produced from photolysis below ~800 km, is recombination to N_2H_4, which along with NH_3 and CH_2NH diffuse downward to the stratosphere.

As mentioned previously, several of the rate coefficients involved in these chemical cycles are uncertain and we therefore consider how the results of the numerical model will change for reasonable variations of these parameters. The parameters for these runs are summarized in Table 2 and the results are shown in Fig. 11. The key reaction for production of NH_3 is R47. Our baseline model uses the calculated rate coefficient described in section 4, which corresponds to a value of 7.4×10^{-11} cm^3 s^{-1} at 150 K (the approximate temperature of Titan's upper atmosphere). The accuracy of the calculated rate coefficient is expected to be 30%, but to be conservative, we also consider in models B and C the consequences of values 50% smaller and larger than our predicted value for the rate coefficient. The results, shown in Fig. 11b reveal that the calculated $CH_2NH_2^+$ density at 1100 km is 30% smaller in model B and 42% larger in model C. The calculated $CH_2NH_2^+$ density does not change significantly for these variations in k_{47}.

The effect of the $CH_2NH_2^+$ recombination rate coefficient is shown in Fig. 11b. Models D and E shows that scaling the net rate coefficient downward by 30% raises the predicted density at 1100 km by 50%, whereas scaling the rate coefficient upward by a factor of 2 lowers the predicted density at 1100 km by 40%. One might suspect that the model would be most sensitive to the branching ratio for production of HCN (R21), because this channel creates a nitrile, thereby removing the N atom from the imine/amine chemistry. However, the density of $CH_2NH_2^+$ in model F does not differ significantly from Model A. We note that none of these variations in the $CH_2NH_2^+$ recombination rate coefficients has a significant effect on the NH_4^+ densities in the models. We also considered uncertainties in the CH_2NH photolysis rate in model G (not shown in Fig. 11). Decreasing this rate by a factor

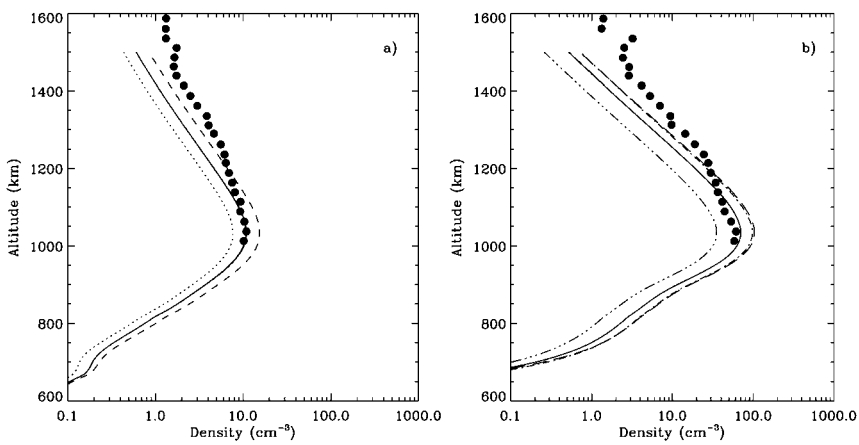

Fig. 11 (a) Calculated NH_4^+ densities for different assumptions about rate coefficients. The data points represent the observations. The solid line represents model A, dotted B, dashed C, dashed-dot D, and dashed-triple dot E. (b) The same as (a), but for $CH_2NH_2^+$.

of 10 caused the CH_2NH density to increase by 20%, which is less than the uncertainty in the data or models. These sensitivity tests support our conclusion that reaction R47 is the primary channel for production of NH_3.

7. Discussion and implications

The distribution of CH_2NH and NH_3 in Titan's upper atmosphere can be understood as the consequence of coupled ion and neutral chemistry. Nitrogen photolysis in Titan's upper atmosphere leads to production of $N(^2D)$ which reacts with CH_4 to either produce CH_2NH directly or produces NH, which reacts with CH_3 to produce CH_2NH. CH_2NH has a large proton affinity, enabling proton-transfer reactions with many species and leading to rapid production of $CH_2NH_2^+$. This ion dissociatively recombines, producing NH_2. Reaction of HCN^+ with C_2H_6 also produces NH_2. Using transition state theory we calculate a rate coefficient for $NH_2 + H_2CN \rightarrow NH_3 + HCN$ of $5.43 \times 10^{-11}(T/300)^{-1.06} \exp(-60.8/T)$. With this coefficient, our photochemical calculations predict densities of NH_4^+ and $CH_2NH_2^+$ in accord with observations.

Much of the nitrogen chemistry used here is based on Lavvas *et al.*[33] and Lavvas *et al.*[10] The important improvements include the detailed treatment of ion chemistry and reaction R47. The lack of ion reactions in Lavvas *et al.*[10] led to an overestimate of the CH_2NH density in those calculations, because of the absence of loss of CH_2NH through proton transfer followed by dissociative recombination. Lavvas *et al.*[10] speculated that CH_2NH may also be lost through radical–radical reactions (for example $CH_2NH + H_2CN$, leading to polymeric molecular growth). This may well be occurring in Titan's atmosphere but measurements or theoretical calculations of the rate coefficients for these processes are required to quantitatively investigate this possibility. The Lavvas *et al.*[10] models also under-predicted the density of NH_3. This is also remedied by ion chemistry through production of the NH_2 molecule from $CH_2NH_2^+$ followed by conversion of NH_2 to NH_3. Thus, the ionospheric chemistry results in the conversion of CH_2NH to NH_3, simultaneously solving both problems encountered with the earlier models.

Photochemical models by Krasnopolsky[11] also predicted CH_2NH mole fractions in fairly good agreement with the observations. CH_2NH is produced by our R29 and loss through $CH_2NH + H \rightarrow CH_3 + NH$ in the Krasnopolsky[11] models; however, this latter reaction is endothermic and unlikely to occur at a significant rate in Titan's atmosphere. Loss through proton-transfer followed by dissociative recombination seems more likely, but is not a dominant process in the Krasnopolsky[11] models because a relatively low value (compared to our value) for the electron recombination rate is assumed. The Krasnopolsky[11] model also under predicts the density of NH_3. The NH_2 densities calculated by Krasnopolsky[11] are consistent with those presented here so the lower NH_3 densities are clearly due to the absence of R47 in those models.

Vuitton *et al.*[12] showed that C_6H_6 in Titan's upper atmosphere was synthesized by a chain of ion–neutral reactions, culminating in dissociative recombination of $C_6H_7^+$, producing C_6H_6. Here, we show that ion chemistry plays a critical role in the chemistry of NH_3 by helping to produce NH_2 from CH_2NH. The Vuitton *et al.*[12] paper and the investigation described herein serve to emphasize the importance of ion chemistry for the composition of the neutral atmosphere. The existence of high energy photons and electrons in the upper atmosphere results in the opening of chemical pathways that are not possible in Titan's stratosphere, where chemistry is instigated by longer wavelength, less energetic solar radiation. This is clearly seen in our models for C_6H_6, NH_3 and CH_2NH chemistry, but is likely to extend beyond these examples and deserves further, careful investigation.

One of the main results of a study such as this is the identification of laboratory measurements required to improve the photochemical models. The most important deficiencies in laboratory data for the chemistry discussed here are the rate

coefficient and products for electron recombination of $CH_2NH_2^+$. In addition, the rate coefficient for $NH_2 + H_2CN \rightarrow NH_3 + HCN$ and the absorption cross section and dissociation products for CH_2NH photodissociation need to be measured.

This research has been supported by the NASA's Planetary Atmospheres Program through grants NNX09AB58G and NNH09AK24I, NASA's exobiology program through grant NNX08AO13G, NASA's Cassini Data Analysis Program through grant NNX08AX62H and NASA Astrobiology Initiative through JPL subcontract 1372177 to the University of Arizona. Computational resources for the kinetics predictions were provided by by the U. S. Department of Energy, Office of Basic Energy Sciences, Division of Chemical Sciences, Geosciences and Biosciences under Contract No. DE-AC02-06CH11357

References

1 T. E. Cravens, I. P. Robertson, J. Clark, J.-E. Wahlund, J. H. Waite, S. A. Ledvina, H. B. Niemann, R. V. Yelle, W. T. Kasprzak, J. G. Luhmann, R. L. McNutt, W.-H. Ip, V. De La Haye, I. Müller-Wodarg, D. T. Young and A. J. Coates, Titan's ionosphere: Model comparisons with Cassini Ta data, *Geophys. Res. Lett.*, 2005, **32**, L12108–12111.
2 V. Vuitton, R. V. Yelle and V. G. Anicich, The nitrogen chemistry of Titan's upper atmosphere revealed, *Astrophys. J.*, 2006, **647**, L175–L178.
3 V. Vuitton, R. V. Yelle and M. J. McEwan, Ion chemistry and N-containing molecules in Titan's upper atmosphere, *Icarus*, 2007, **191**, 722–742.
4 S. M. Hörst, , R. V. Yelle, , A. Bauch, , N. Carrasco, , G. Cernogora, , O. Dutuit, , E. Quirico, , E. Sciamma-O B'rien, , M. A. Smith, , A. Somogyi, , C. Szopa, , R. Thissen and and V. Vuitton, , Formation of prebiotic molecules in a Titan simulation experiment, in preparation.
5 J. L. Fox and R. V. Yelle, Hydrocarbon ions in the ionosphere of Titan, *Geophys. Res. Lett.*, 1997, **24**, 2179–2182.
6 Y. L. Yung, M. Allen and J. P. Pinto, Photochemistry of the atmosphere of Titan – comparison between model and observations, *Astrophys. J. Suppl.*, 1984, **55**, 465–506.
7 D. Toublanc, J. P. Parisot, J. Brillet, D. Gautier, F. Raulin and C. P. McKay, Photochemical modeling of Titan's atmosphere, *Icarus*, 1995, **113**, 2–26.
8 L. M. Lara, E. Lellouch, J. J. López-Moreno and R. Rodrigo, Vertical distribution of Titan's atmospheric neutral constituents, *J. Geophys. Res.*, 1996, **101**, 23261–23283.
9 E. H. Wilson and S. K. Atreya, Current state of modeling the photochemistry of Titan's mutually dependent atmosphere and ionosphere, *J. Geophys. Res.*, 2004, **109**, E06002.
10 P. P. Lavvas, A. Coustenis and I. M. Vardavas, Coupling photochemistry with haze formation in Titan's atmosphere, Part II: Results and validation with Cassini–Huygens data, *Planet. Space Sci.*, 2008, **56**, 67–99.
11 V. A. Krasnopolsky, A photochemical model of Titan's atmosphere and ionosphere, *Icarus*, 2009, **201**, 226–256.
12 V. Vuitton, R. V. Yelle and J. Cui, Formation and distribution of benzene on Titan, *J. Geophys. Res.*, 2008, **113**, E05007.
13 J. Cui, M. Galand, R. V. Yelle, V. Vuitton, J. Wahlund, P. P. Lavvas, I. C. F. Müller-Wodarg, T. E. Cravens, W. T. Kasprzak and J. H. Waite, Diurnal variations of Titan's ionosphere, *J. Geophys. Res.*, 2009, **114**, A06310.
14 J. Cui, M. Galand, R. V. Yelle, J. Wahlund, K. Ångren, J. H. Waite and M. K. Dougherty, Ion transport in Titan's upper atmosphere, *J. Geophys. Res.*, 2010, in press.
15 K. Ågren, J. Wahlund, P. Garnier, R. Modolo, J. Cui, M. Galand and I. Müller-Wodarg, On the ionospheric structure of Titan, *Planet. Space Sci.*, 2009, **57**, 1821–1827.
16 S. K. Atreya, *Atmospheres and Ionospheres of the Outer Planets and their Satellites*, 1986, Springer-Verlag.
17 P. Lavvas, M. Galand, R. V. Yelle, A. N. Heays, B. R. Lewis, G. R. Lewis and A. J. Coates, 2010, , Energy deposition a primary chemical products in Titan's upper atmosphere, in preparation.
18 M. T. Nguyen, D. Sengupta and T. K. Ha, Another look at the decomposition of methyl azide and methanimine: how is HCN formed?, *J. Phys. Chem.*, 1996, **100**, 6499–6503.
19 T. H. Dunning, Jr., Gaussian basis sets for use in correlated molecular calculations. I. The atoms boron through neon and hydrogen, *J. Chem. Phys.*, 1989, **90**, 1007–1023.
20 R. A. Kendall, T. H. Dunning, Jr. and R. J. Harrison, Electron affinities of the first-row atoms revisited. Systematic basis sets and wave functions, *J. Chem. Phys.*, 1992, **96**, 6796–6806.

21 S. J. Klippenstein, Variational optimizations in the Rice–Ramsperger–Kassel–Marcus theory calculations for unimolecular dissociations with no reverse barrier, *J. Chem. Phys.*, 1992, **96**, 367–371.
22 Y. Georgievskii and S. J. Klippenstein, Variable reaction coordinate transition state theory: Analytic results and application to the $C_2H_3 + H \rightarrow C_2H_4$ reaction, *J. Chem. Phys.*, 2003, **118**, 5442–5455.
23 S. J. Klippenstein, A. L. L. East and W. D. Allen, A high level ab initio map and direct statistical treatment of the fragmentation of singlet ketene, *J. Chem. Phys.*, 1996, **105**, 118–140.
24 S. J. Klippenstein and L. B. Harding, A theoretical study of the kinetics of $C_2H_3 + H$, *Phys. Chem. Chem. Phys.*, 1999, **1**, 989–997.
25 L. B. Harding, Y. Georgievskii and S. J. Klippenstein, Predictive theory for hydrogen atom–hydrocarbon radical association kinetics, *J. Phys. Chem. A*, 2005, **109**, 4646–4656.
26 S. J. Klippenstein, Y. Georgievskii and L. B. Harding, Predictive theory for the combination kinetics of two alkyl radicals, *Phys. Chem. Chem. Phys.*, 2006, **8**, 1133.
27 P. Celani and H. Werner, Multireference perturbation theory for large restricted and selected active space reference wave functions, *J. Chem. Phys.*, 2000, **112**, 5546–5557.
28 R. D. Amos, A. Bernhardsson, A. Berning, P. Celani, D. L. Cooper, M. J. O. Deegan, A. J. Dobbyn, F. Eckert, C. Hampel, G. Hetzer, P. J. Knowles, T. Korona, R. Lindh, A. W. Lloyd, S. J. McNicholas, F. R. Manby, W. Meyer, M. E. Mura, A. Nicklass, P. Palmieri, R. Pitzer, G. Rauhut, M. Schütz, U. Schumann, H. Stoll, A. J. Stone, R. Tarroni, T. Thorsteinsson and H.-J. Werner, *MOLPRO, a package of* ab initio *programs designed by H.-J. Werner and P. J. Knowles, Version 2009.1*, 2009.
29 H. Werner and P. J. Knowles, A second order multiconfiguration SCF procedure with optimum convergence, *J. Chem. Phys.*, 1985, **82**, 5053–5063.
30 P. J. Knowles and H. Werner, An efficient second-order MC SCF method for long configuration expansions, *Chem. Phys. Lett.*, 1985, **115**, 259–267.
31 M. J. Frisch, G. W. Trucks, H. B. Schlegel, G. E. Scuseria, M. A. Robb, J. R. Cheeseman, V. G. Zakrzewski, J. A. Montgomery, Jr., R. E. Stratmann, J. C. Burant, S. Dapprich, J. M. Millam, A. D. Daniels, K. N. Kudin, M. C. Strain, O. Farkas, J. Tomasi, V. Barone, M. Cossi, R. Cammi, B. Mennucci, C. Pomelli, C. Adamo, S. Clifford, J. Ochterski, G. A. Petersson, P. Y. Ayala, Q. Cui, K. Morokuma, D. K. Malick, A. D. Rabuck, K. Raghavachari, J. B. Foresman, J. Cioslowski, J. V. Ortiz, A. G. Baboul, B. B. Stefanov, G. Liu, A. Liashenko, P. Piskorz, I. Komaromi, R. Gomperts, R. L. Martin, D. J. Fox, T. Keith, M. A. Al-Laham, C. Y. Peng, A. Nanayakkara, C. Gonzalez, M. Challacombe, P. M. W. Gill, B. G. Johnson, W. Chen, M. W. Wong, J. L. Andres, M. Head-Gordon, E. S. Replogle and J. A. Pople, *GAUSSIAN 98*, Gaussian, Inc., Pittsburgh, PA, 1998.
32 S. M. Hörst, V. Vuitton and R. V. Yelle, Origin of oxygen species in Titan's atmosphere, *J. Geophys. Res.*, 2008, **113**, E10006.
33 P. P. Lavvas, A. Coustenis and I. M. Vardavas, Coupling photochemistry with haze formation in Titan's atmosphere, Part I: Model description, *Planet. Space Sci.*, 2008, **56**, 27–66.
34 E. A. Mason, and T. R. Marrero, The diffusion of atoms and molecules, in *Advances in Atomic and Molecular Physics*, 1970, vol. 6, pp. 155–232.
35 W. J. Massman, A review of the molecular diffusivities of H_2O, CO_2, CO, O_3, SO_2, NH_3, N_2O, NO and NO_2 in Air, O_2, and N_2 near STP, *Atmos. Environ.*, 1998, **32**, 1111–1127.
36 R. V. Yelle, J. Cui and I. C. F. Müller-Wodarg, Methane escape from Titan's atmosphere, *J. Geophys. Res. [Planets]*, 2008, **113**, 10003.
37 I. C. F. Müller-Wodarg, R. V. Yelle, J. Cui and J. H. Waite, Horizontal structures and dynamics of Titan's thermosphere, *J. Geophys. Res.*, 2008, **113**, E10005.
38 J. A. R. Samson, T. Masuoka, P. N. Pareek and G. C. Angel, Total and dissociative photoionization cross sections of N_2 from threshold to 107 eV, *J. Chem. Phys.*, 1987, **86**, 6128–6132.
39 W. C. Stolte, Z. X. He, J. N. Cutler, Y. Lu and J. A. R. Samson, Dissociative photoionization cross sections of N_2 and O_2 from 100 to 800 eV, *At. Data Nucl. Data Tables*, 1998, **69**, 171.
40 A. Teslja, B. Nizamov and P. J. Dagdigian, The electronic spectrum of methyleneimine, *J. Phys. Chem.*, 2004, **108**, 4433–4439.
41 F. Z. Chen, D. L. Judge, C. Y. R. Wu and J. Caldwell, Low and room temperature photoabsorption cross sections of NH_3 in the UV region, *Planet. Space Sci.*, 1999, **47**, 261–266.
42 B. M. Cheng, H. C. Lu, H. K. Chen, M. Bahou, Y. P. Lee, A. M. Mebel, L. C. Lee, M. C. Liang and Y. L. Yung, Absorption cross sections of NH_3, NH_2D, NHD_2, and

ND_3 in the spectral range 140–220 nm and implications for planetary isotopic fractionation, *Astrophys. J.*, 2006, **647**, 1535–1542.
43 V. G. Anicich, Evaluated bimolecular ion–molecule gas phase kinetics of positive ions for use in modeling planetary atmospheres, cometary comae, and interstellar clouds, *J. Phys. Chem. Ref. Data*, 1993, **22**, 1469–1569.
44 V. G. Anicich and M. J. McEwan, Ion–molecule chemistry in Titan's ionosphere, *Planet. Space Sci.*, 1997, **45**, 897–921.
45 M. J. McEwan, G. B. I. Scott and V. G. Anicich, Ion–molecule reactions relevant to Titan's ionosphere, *Int. J. Mass Spectrom. Ion Processes*, 1998, **172**, 209–219.
46 S. J. Edwards, C. G. Freeman and M. J. McEwan, The ion chemistry of methylenimine and propionitrile and their relevance to Titan. Inter. J., *Int. J. Mass Spectrom.*, 2008, **272**, 86–90.
47 S. Petrie, C. G. Freeman and M. J. McEwan, The ion-molecule chemistry of acrylonitrile – astrochemical implications, *Mon. Not. R. Astron. Soc.*, 1992, **257**, 438–444.
48 J. Öjekull, P. U. Andersson, M. B. Nagard, J. B. C. Pettersson, A. M. Derkatch, A. Neau, S. Rosén, R. Thomas, M. Larsson, F. Österdahl, J. Semaniak, H. Danared, A. Källberg, M. a. Ugglas and N. Markovicć, Dissociative recombination of NH_4^+ and ND_4^+ ions: Storage ring experiments and ab initio molecular dynamics, *J. Chem. Phys.*, 2004, **120**, 7391–7399.
49 S. Dobe, C. Oehlers, F. Temps, H. G. Wagner and H. Ziemer, Observations of an H/D-isotope exchange channel in the reaction D + H_2CO, *Ber. Bunsen-Ges. Phys. Chem.*, 1994, **98**, 754–757.
50 G. Marston, F. L. Nesbitt and L. J. Stief, Branching ratios in the N + CH_3 reaction – Formation of the methylene amidogen (H_2CN) radical, *J. Chem. Phys.*, 1989, **91**, 3483–3491.
51 F. L. Nesbitt, G. Marston and L. J. Stief, Kinetic studies of the reactions of H_2CN and D_2CN radicals with N and H, *J. Phys. Chem.*, 1990, **94**, 4946–4951.
52 H. Okabe, *Photochemistry of Small Molecules*, 1978, John Wiley and Sons Inc., New York.
53 J Herron, Evaluated chemical kinetics data for reactions of N(^{2}D) N(^{2}P), and $N_2(A^3\Sigma^+_u)$ in the gas phase, *J. Phys. Chem. Ref. Data*, 1999, **28**, 1453.
54 H. Umemoto, T. Nakae, H. Hashimoto, K. Kongo and M. Kawasaki, Reactions of N(^{2}D) with methane and deuterated methanes, *J. Chem. Phys.*, 1998, **109**, 5844–5848.
55 N. Balucani, O. Asvany, Y. Osamura, L. C. L. Huang, Y. T. Lee and R. I. Kaiser, Laboratory investigation on the formation of unsaturated nitriles in Titan's atmosphere, *Planet. Space Sci.*, 2000, **48**, 447–462.
56 L. Adam, W. Hack, H. Zhu, Z.-W. Qu and R. Schinke, Experimental and theoretical investigation of the reaction NH($X^3\Sigma^-$) + H(^{2}S) → N(^{4}S) + $H_2(X^1\Sigma_g^+)$, *J. Chem. Phys.*, 2005, **122**(11), 114301.
57 C. Mullen and M. A. Smith, Low temperature NH($X^3\Sigma^-$) radical reactions with NO, saturated, and unsaturated hydrocarbons studied in a pulsed supersonic laval nozzle flow reactor between 53 and 188 K, *J. Phys. Chem.*, 2005, **109**, 1391–1399.
58 W. Hack, H. Wagner and A. Zaspypkin, Elementary reactions of NH($^1\Delta$) and NH($X^3\Sigma$) with N, O and NO, *Bunsen-Ges. Phys. Chem.*, 1994, **98**, 156–164.
59 Z.-F. Xu, F. D.-C. and F.X.-Y, Ab initio study on the reaction 2NH($X^3\Sigma^-$) → $NH_2(X^2B_1)$ + N(^{4}S), *Chem. Phys. Lett.*, 1997, **275**(3–4), 386–391.
60 P. Dransfeld and H. G. Wagner, Investigation of the gas phase reaction N + NH_2 → N_2 + 2H, *Z. Phys. Chem., Neue Folge*, 1987, **153**, 89–97.
61 K. Fagerstrom, J. T. Jodkowski and E. Ratajczak, Kinetics of the self-reaction and the reaction with OH of the amidogen radical, *Chem. Phys. Lett.*, 1995, **236**, 103–110.
62 M. Liang, A. N. Heays, B. R. Lewis, S. T. Gibson and Y. L. Yung, Source of nitrogen isotope anomaly in HCN in the atmosphere of titan, *Astrophys. J.*, 2007, **664**, L115–L118.
63 B. R. Lewis, S. T. Gibson, J. P. Sprengers, W. Ubachs, A. Johansson and C. Wahlström, Lifetime and predissociation yield of $^{14}N_2$ $b^1\Pi_u$ ($v = 1$) revisited: Effects of rotation, *J. Chem. Phys.*, 2005, **123**(23), 236101.
64 J. Cui, R. V. Yelle, V. Vuitton, J. H. Waite, W. T. Kasprzak, D. A. Gell, H. B. Niemann, I. C. F. Müller-Wodarg, N. Borggren, G. G. Fletcher, E. L. Patrick, E. Raaen and B. A. Magee, Analysis of Titan's neutral upper atmosphere from Cassini ion neutral mass spectrometer measurements, *Icarus*, 2009, **200**, 581–615.
65 S. Petrie, G. Javahery and D. K. Bohme, Gas-phase reactions of benzenoid hydrocarbon ions with hydrogen atoms and molecules: uncommon constraints to reactivity, *J. Am. Chem. Soc.*, 1992, **114**, 9205.